J Surg Res 2021; 4 (1): 128-141 *DOI: 10.26502/jsr.10020117*

Research Article

Carboxymethylcellulose Activates Dermal Cells and Adipose-Derived Stem Cells Through Wnt/β-catenin Pathway

Dongyi Peng[1,2], Amanda B. Reed-Maldonado[1,3], Lia Banie[1], Guifang Wang[1], Guiting Lin[1] and Tom F. Lue[1*]

[1]Knuppe Molecular Urology Laboratory, Department of Urology, School of Medicine, University of California, San Francisco, CA 94143, USA

[2]Center of Andrology, Department of Urology, the Third Xiangya Hospital of Central South University

[3]Department of Urology, Tripler Army Medical Center, 1 Jarrett White Road, Honolulu, HI. 96859, USA

[*]Corresponding Author: Tom F. Lue MD, Department of Urology, University of California, San Francisco, 400 Parnassus Ave., Ste A-630, San Francisco, CA 94143-0738, USA, Phone (O): 415-476-1611, Fax: 415-476-3803.

Received: 26 Febrauary 2021; **Accepted:** 06 March 2021; **Published:** 15 March 2021

Citation: Dongyi Peng, Amanda B. Reed-Maldonado, Lia Banie, Guifang Wang, Guiting Lin and Tom F. Lue. Carboxymethylcellulose Activates Dermal Cells and Adipose-Derived Stem Cells Through Wnt/β-catenin Pathway. Journal of Surgery and Research 4 (2021): 128-141.

Abstract

Background: Carboxymethylcellulose (CMC) is an inexpensive biomaterial that has been used for wound dressings and as an excipient for drug therapy. CMC in combination with adipose-derived stem cells has been reported to enhance tissue healing. The mechanisms underlying this effect are poorly understood.

Objective: To investigate the effects of CMC and BloodSTOP iX (BSiX) on porcine dermal cells (PDCs) and porcine adipose-derived stem cells (PADSCs) to define the mechanisms of CMC in activating PDCs and PADSCs.

Methods: A young pig was used to isolate PDCs and PADSCs. PDCs were treated with different concentrations of CMC, BloodSTOP (BS), and BSiX. Expression of phosphorylated histone 3 (H3P) and cell proliferation were then assessed. To explore the mechanisms of CMC in activating PDCs and PADSCs, the cells were treated with different concentrations of CMC (0,10,100,1000μg/ml), and Western blot was used

to measure the proteins of the Wnt/β-catenin pathway.

Results: CMC and BSiX had significant effects in promoting PDC cell growth, while the effect of BS was minor. Both CMC and BSiX promoted PDCs mitosis in vitro; BSiX at a concentration of 100μg/ml had the best effect. Both CMC and BSiX promoted PDC proliferation in a dose-dependent manner, but the effect from BSiX was much greater than that of CMC. CMC activated AMPK in both PDCs and PADSCs. AMPK by crosstalking with Wnt/β-catenin, activated AMPK promotes the expression of its downstream genes, such as H3P and Cyclin D1.

Conclusion: We successfully isolated and cultured PDCs and PADSCs. We found that both CMC and BSiX promoted PDC mitosis and proliferation in a dose-dependent manner. In both PDC and PADSC, CMC activated Wnt/β-catenin signaling pathway through AMPK. This could be the underlying mechanism by which CMC activates stem cells and dermal cells to promote wound healing.

Keywords: Carboxymethylcellulose; Porcine dermal cells; Adipose-derived stem cells; Wnt/β-catenin Pathway; Activation of stem cells

1. Introduction

Sodium carboxymethyl cellulose (CMC) is synthesized through the hydration reaction of cellulose and sodium hydroxide and the catalytic reaction of alkaline pulp and chloroacetic acid. CMC is a well-known, inexpensive, available biomaterial that has been employed for wound dressings with the dual purposes of wound protection and as an excipient for drug therapy [1]. The surfaces of dressings are responsible for important interactions of biomaterials since they create an interface with the biological environment and affect the response that the body will have to the material. Researches demonstrated that surface roughness and morphology have great impact on the material performance, affecting cellular, bacterial, and biomolecular adhesion [2, 3]. It has been proven that the therapeutic concentration of CMC used in wound dressings is safe and does not interfere with cellular function [4, 5].

BloodSTOP (BS) and BloodSTOP iX (BSiX) are the most advanced forms of CMC, and they have been widely utilized in wound care [6]. This synthetic polymer has been shown to be suitable for hemostatic application, wound sealing, and wound protection for skin wounds such as burns [7]. Very recently, it was noted that this polymer promotes adipose-derived stem cell (ADSC) proliferation and enhances wound healing [4]. More interestingly, CMC binds to the epithelium and promotes cell migration for tissue regeneration [8, 9]. Commonly utilized for partial thickness wounds [6], diabetic ulcers, lesions of the foot, and deep dermal fillers [10, 11], CMC and BSiX may be applied alone or as an excipient for drug therapy.

In recent years, many studies have investigated methods to improve CMC as a biomaterial in order to explore its potential applications in tissue bioengineering. One study [5] developed CMC microparticles through ionic crosslinking with the aqueous ion complex of zirconium (Zr) confirmed by Fourier transform infrared spectroscopy results (FTIR). The authors found that Zr enhances the surface roughness of the microparticles and increases the stability of microparticles in phosphate buffer. CMC has also been used to form a new hybrid material (CMC-HA) containing HA in CMC-based hydrogel. CMC-HA was found to enhance cellular proliferation and metabolic activity and to

promote the production of mineralized extracellular matrix [12]. There are also many different material forms of CMC including dialdehyde carboxymethyl (DCMC) [13], silver nanoparticles, and carboxymethylcellulose (SNPs-CMC) [14], silver nanoparticles (AgNPs)-loaded CMC hydrogel [15], and CMC derivative bearing phenolic hydroxyl groups (CMC-Ph) [16]. For instance, BloodStop is a thin CMC film that is nontoxic and biocompatible with the human cells. It has been shown to have the biomedical potential to promote cell proliferation and cell growth [17]. After injury to the skin, a new epithelium must form in order to repair the wound. This process requires proliferation of keratinocytes, fibroblasts, dermal stem cells (DSCs), and mesenchymal stem cells (MSCs). Essential for skin homeostasis and wound healing, DSCs and MSCs promote cell differentiation and re-epithelialization. In 2008, we first localized tissue-resident adipose-derived stem cells (ADSCs) in situ [18]. Subsequent studies indicated that ADSCs possess the ability to regenerate many types of tissues [19, 20]. In 2014, Dr. Cristiano Rodrigues et al explored the effect of CMC on ADSCs for tissue healing and demonstrated that CMC significantly enhanced tissue healing when combined with ADSC in a rat skin injury model [4]. When treated with CMC 10 µg/ml plus ADSC, there was a significant increase in epithelial cell proliferation after 4 days and an increase in epithelium thickness after 8 days. Such an improvement at the histological level may be particularly important in large wounds, which cause the greatest morbidity and carry the greatest risk of mortality.

The underlying mechanisms for the findings of improved wound healing with the combination of CMC plus ADSC remain poorly understood. In this study, we isolated porcine dermal cells (PDCs) and porcine adipose-derived stem cells (PADSCs), and we treated those cells with CMC, BS, and BSiX. Cell proliferation, mitosis, and cellular signaling pathways with the goal of further defining these mechanisms.

2. Materials & Methods

2.1. Isolation of PDCs and PADSCs

Experiments were approved by the Institutional Animal Care and Use Committee at the University of California, San Francisco. Porcine dermal tissues were morcellated into small pieces in PBS on ice then complete dispase (0.8U/ml) in RPMI1640 was added for 5 times volume. After incubating at 4°C overnight, the tissues were next incubated at 37°C for 2 hours allowing for the dissection of dermis from epidermis with tweezers. The dermis was then incubated separately in 0.1% collagenase D in complete RPMI 1640 medium at 37°C overnight. After vigorously pipetting the dermal solution to single cell suspension, the cell suspension was filtered with a 70-µm filter. The cells were then cultured in DMEM containing 10% FBS, 1% Pen/Strep, 1% ascorbic acid, and 10ng/ml EGF and FGF2.

The procedure of ADSC isolation has been described previously [19]. Briefly, the adipose tissue was rinsed with PBS containing 1% penicillin and streptomycin, minced into small pieces, then incubated in a solution containing 0.075% collagenase type IA (Sigma-Aldrich, St. Louis, MO) for 1 hour at 37°C with vigorous agitation. The top lipid layer was removed, and the remaining liquid portion was centrifuged at 220 g for 10 minutes at room temperature. The pellet was treated with 160 mM NH_4Cl for 10 min to lyse red blood cells. The remaining cells were suspended in DMEM supplemented with 10% fetal bovine serum (FBS), filtered through a 40-µm cell strainer (BD Biosciences, Bedford, MA), and plated at a density of 1

× 106 cells in a 10-cm dish. After reaching 80% confluence, the cells were harvested and stored in liquid nitrogen at a density of 5 x 105 cells per ml of freezing media (DMEM, 20% FBS, and 10% DMSO). The frozen cells were thawed for experiments as needed.

2.2. Preparation of CMC, BS, and BSiX.

CMC (C9481, Sigma-Aldrich, Inc), BS (LifeScience Plus. Inc) and BSiX (LifeScience Plus. Inc) were used in this experiment. The reagents were dissolved in PBS, filtered with 200 um filter, and stored at 4°C.

2.3. In vitro binding of CMC, BS, and BSiX to PDCs

PDCs were seeded in 6-well plates (covered with glass cover slides) and cultured overnight in DMEM supplemented with 10% FBS. This was followed by treatment with CMC, BS, and BSiX. This concentration of CMC, BS and BSiX or controls was selected as 100µg/ml. The cells were cultured in test media for 24 hours. At the end of culture, the cells were washed extensively with culture medium to remove the unbound CMC, BS, and BSiX. The cells were then labeled with 10uM Calcein-AM to view the fluorescence density and cell numbers.

2.4. Treatment of PDCs and PADSCs with CMC and BSiX.

PDCs and PADSCs at 80% confluence were rinsed twice with PBS, trypsinized, and resuspended in serum-free DMEM (supplemented with 0.1% BSA) at 1 × 105 cells/ml. For the cell mitosis assay, the cells were seeded into 6 well dishes (with glass cover slides). For the cell proliferation assay, the cells were seeded into 96 well dishes. For the cellular signaling assay, the cells were seeded in 6 well dishes. Before each experiment, the cells were treated with in serum-free DMEM (supplemented with 0.1% BSA) for cell synchronization. The PDCs and PADSCs were then treated with different concentrations of CMC (0,10,100,1000µg/ml) or BSiX (0,10,100,1000µg/ml) for different time points.

2.5. Cell proliferation assay with MTT

The effect of CMC, BS, and BSiX on cell proliferation was assayed with the CellTiter-96 kit (Promega Inc, Madison, WI). All the reagents were dissolved in PBS at 1000 mg/ml as stock solution; further dilutions were made in serum-free DMEM supplemented with 0.1% BSA. Each of the PDCs or PADSCs was assayed in one flat-bottom 96-well cell culture plate. To assay the dose-dependent response, the 12 columns of the plate were divided into four groups that received 0, 10, 100 and 1000 µg/ml of CMC, BS and BSiX per well, respectively.

Cells at 80% confluence were rinsed twice with PBS, trypsinized, and resuspended in serum-free DMEM (supplemented with 0.1% BSA) at 105 cells/ml. Aliquots of 50µL of the cell suspension were then transferred to the 96-well plate so that each well contained 5000 cells in a final volume of 100µL, with reagent concentrations of 0–1000µg/ml. The plate was incubated at 37°C in a humidified incubator with 5% CO2; 24 h later 20µL of CellTiter 96 AQueous One Solution Reagent was added to each well. After 2 h of further incubation at 37°C in the humidified 5% CO2 incubator, color development, which reflects cell number, was recorded with a plate reader (MolecularDevices Corp., Sunnyvale, CA) at 490-nm absorbency.

For the time-course assay, the procedure was similar except that a fixed concentration of 100µg/L was used, and the cells were allowed to incubate for 0, 24, 48, 72,

and 96 h after treatment. All assays were duplicated in each experiment, and all data presented as the mean of three independent experiments.

2.6. Western blot for cellular signaling assay

The cellular protein samples were prepared by homogenization of cells in a lysis buffer containing 1% IGEPAL CA-630, 0.5% sodium deoxycholate, 0.1% sodium dodecyl sulfate, aprotinin (10mg/ml), leupeptin (10mg/ml), and PBS. Cell lysates containing 20μg of protein were electrophoresed in sodium dodecyl sulfate polyacrylamide gel electrophoresis and then transferred to a polyvinylidene fluoride membrane (Millipore Corp, Bedford, MA). The membrane was stained with Ponceau S to verify the integrity of the transferred proteins and to monitor the unbiased transfer of all protein samples. Detection of target proteins on the membranes was performed with an electrochemiluminescence kit (Amersham Life Sciences Inc, Arlington Heights, IL) with the use of primary antibodies for p-AMPK(Thr172) (1:500), AMPK (1:300) (Cell Signaling Technology, Beverly, MA), β-catenin (1:500), cyclin D1 (1:500), and β-actin (1:1000) (Santa Cruz Biotechnology, Santa Cruz, CA). After the hybridization of secondary antibodies, the resulting images were analyzed with the ChemiImager 4000 (Alpha Innotec) to determine the integrated density value of each protein band.

2.7. Immunofluorescence staining for cell mitosis assay

The cells were fixed with ice-cold methanol for 8min, permeabilized with 0.05% TritonX-100 for 5min, and blocked with 5% normal HS in PBS for 1h at room temperature. Next, they were incubated with rabbit anti-H3P (1:500, Merck Millipore, Billerica, MA, USA) antibody for 1h at room temperature. After washing with PBS three times, the cells were incubated with Alexa Fluor-conjugated goat anti-rabbit antibody (1:500, Invitrogen Inc) for 1h at room temperature. After three washes with PBS, the cells were stained with DAPI for 5 min for nuclear staining. Finally, the immunofluorescence slides were examined under a fluorescence microscope and photographed.

2.8. Statistical analysis

Data were analyzed with Prism 5 (GraphPad Software, San Diego, CA) and presented as means ± standard deviation (S.D). Statistical significance between two groups was analyzed by the Student t-test. For statistical significance among multiple groups, one-way ANOVA analysis followed by Bonferroni post hoc analysis was performed.

3. Results

3.1. CMC, BS and BSiX promoted PDC growth in vitro

To test the effects of CMC, BS, and BSiX on cell growth, based on our preliminary data, we selected a concentration of 100μg/ml to treat the cells for 24 hr. Both CMC and BSiX had significant effects in promoting cell growth, with BSiX having a greater impact on cell growth (Figure 1). The effect from BS was minor.

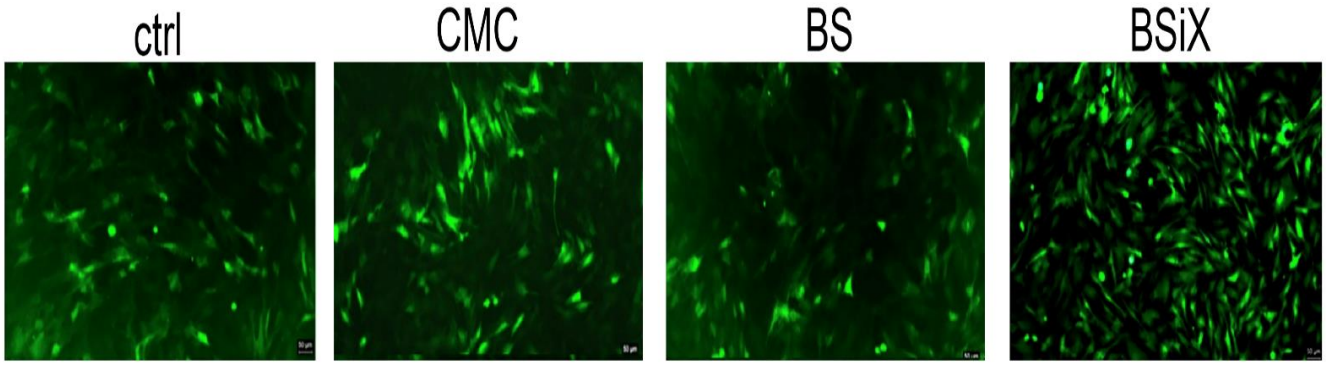

Figure 1: PDCs growth after treatment with CMC, BS, and BSiX in vitro

3.2. CMC and BSiX promoted PDC mitosis in vitro

Based on the result from the above experiment, we also assessed cell mitosis by evaluating H3P in the cells after CMC and BSiX treatment at high and low concentrations of 1000μg/ml and 100 μg/ml, respectively. With CMC and BSiX treatment, more cells underwent mitosis and expressed high H3P (Figure 2). In the control group, the percentage of cells undergoing mitosis (percentage of H3P positive) was 4.8±0.6%. This increased to 22.2±3.5% in the BSiX 100μg/ml group ($P<0.01$), 12.5±3.2% in CMC 100μg/ml group ($P<0.05$), 13.2±2.2% in BSiX 1000μg/ml group ($P<0.05$), and 11.9±3.6% in CMC 1000μg/ml group ($P<0.05$). Interestingly, there were more cells in mitosis in the BSiX 100μg/ml group than in the CMC 100μg/ml group ($P<0.05$) while there was no significant difference between the CMC 1000μg/ml group or the BSiX 1000μg/ml.

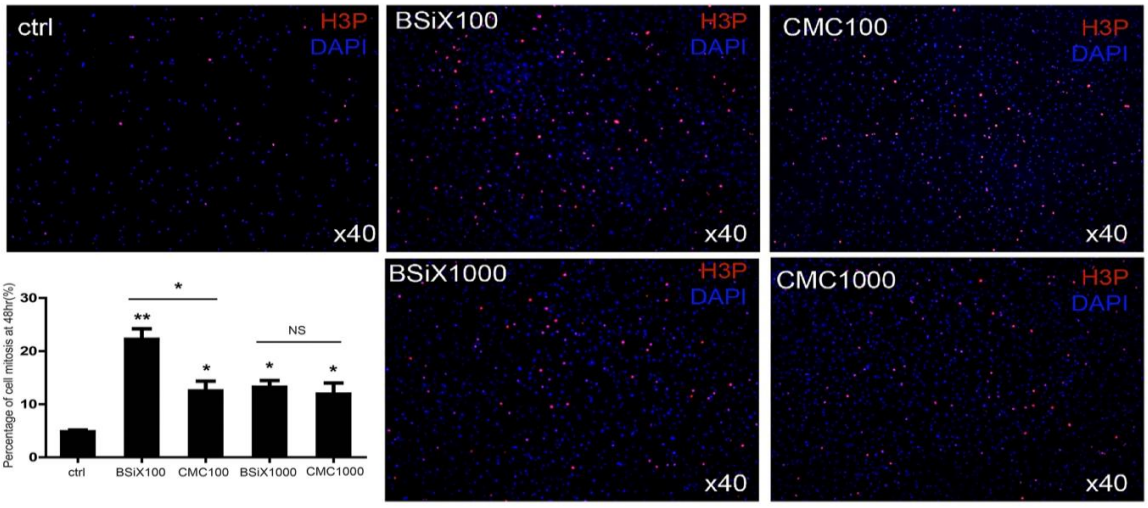

Figure 2: PDCs mitosis enhanced by CMC and BSiX treatment in vitro. After treatment, mitosis in treated groups was increased compared to the control. Interestingly, there were more cells in mitosis in the BSiX 100μg/ml group than in the CMC 100μg/ml group, while there were no significant differences between 1000μg/ml groups of CMC and BSiX (n=3, error bars represent SD, *P< 0.05, **P< 0.01).

3.3. Differential increased PDC proliferation after treatment with CMC and BSiX

After treatment with CMC and BSiX at 0, 10, 100, and 1000μg/ml, PDC growth was significantly increased in different time point. More interesting, PDC increased in a dose-dependent manner with BSiX treatment.

MTT was used to assay PDC proliferation after CMC treatment. As shown in Figure. 3a, At timepoints of 24,48, 72, and 96 hours, the increase of cell number was significant ($P < 0.05$ and $P< 0.01$), but there were no difference of cell number between the different concentration CMC groups. The cell doubling time was then calculated; CMC with all concentration reduced the SC doubling time from ($P < 0.01$) (Figure 3b).

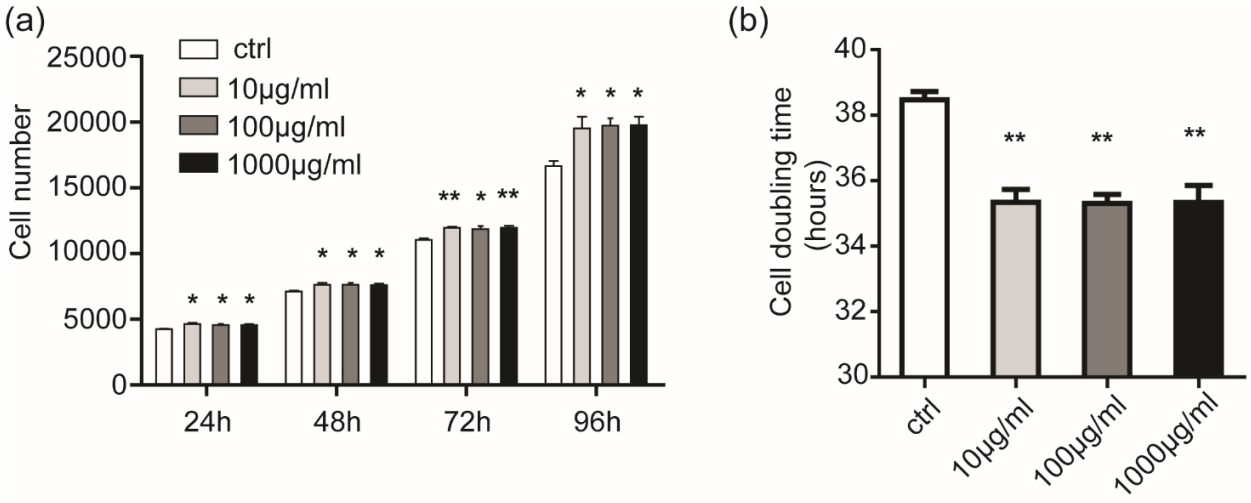

Figure 3: PDCs proliferation affected by CMC at different concentration in vitro. (a). CMC increased the cell number of PDCs at timepoints of 24,48, 72, and 96 hours ($P < 0.05$ and $P< 0.01$). (b). CMC reduced The cell doubling time of PDCs . (n=3, error bars represent SD, *P< 0.05, **P< 0.01)

After treatment of BSiX, the increase of cell number was significant and peak at 100μg/ml at timepoints of 24,48, 72, and 96 hours, ($P < 0.05$ and $P< 0.01$, Figure 4a). Meanwhile, the increase at 100μg/ml was higher than others, which means BSiX promote PDCs proliferation in a dose-dependent manner. Moreover, the BSiX with all concentration reduced the SC doubling time ($P < 0.01$ and $P< 0.01$) (Figure 4b). Then, we compare the cell number between CMC (100μg/ml) and BSiX(100μg/ml) at all time point. As showed in Figure 4c, the effect of BSiX(100μg/ml) was stronger than CMC (100μg/ml).

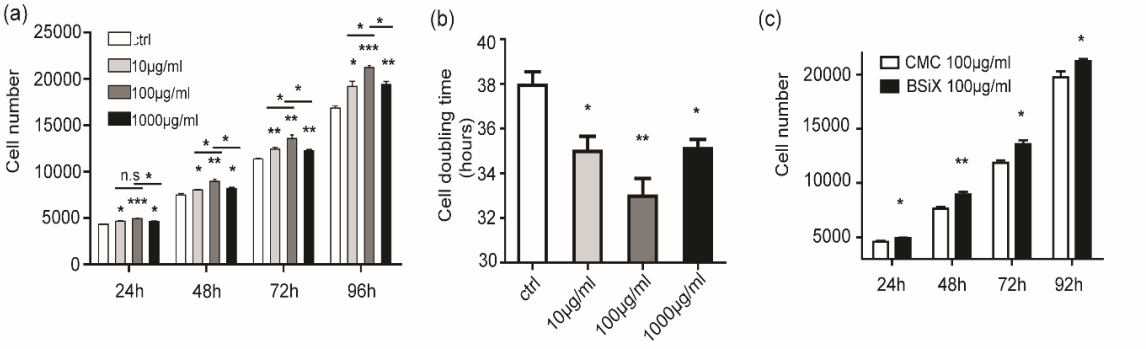

Figure 4: PDCs proliferation affected by BSiX at different concentration in vitro. (a). BSiX increased the cell number of PDCs at timepoints of 24,48, 72, and 96 hours in a dose-dependent manner and peak at 100μg/ml. (b). BSiX reduced the cell doubling time of PDCs. (c)The increase of cells number was higher in BSiX(100μg/ml) than CMC (100μg/ml). (n=3, error bars represent SD, n.s: no significance, *P< 0.05, **P< 0.01).

3.4. CMC activates the Wnt/β-catenin signal pathway through activation of AMPK

It is well known that the Wnt/β-catenin signal pathway is the pivotal pathway in stem cell activation. To explore the mechanisms by which CMC promotes cell PDC and PADSC proliferation, we assessed the Wnt/β-catenin signal pathway and its related proteins after treatment with difference concentrations of CMC.

As shown in Figure 5a, CMC enhanced the phosphorylation of AMPK, which led to the accumulation of β-catenin and activated the Wnt/β-catenin signal pathway. This resulted in increased expression of cyclin D1 in both PDCs and PADSCs. In the PDCs after 48 hours of stimulation, the phosphorylation level of AMPK was 12.89±1.19% in the control group, increased to 20.33±1.78% ($p < 0.05$) in the CMC 10μg/ml group, to 22.27±1.55%($p < 0.01$) in the CMC 100μg/ml group, and to 21.69±1.37%($p < 0.05$) in the CMC 1000μg/ml group. While the β-catenin/β-actin ratio was 0.45±0.05 in the control group, increased to 0.75±0.05% ($p < 0.01$) in the CMC 10μg/ml group, to 0.92±0.03% ($p < 0.01$) in the CMC 100μg/ml group, and 0.85±0.08% ($p < 0.05$) in the CMC 1000μg/ml group. The cyclin D1/β-actin ratio was 0.38±0.03 in the control group, increased to 0.61±0.05% ($p < 0.05$) in the CMC 10μg/ml group, to 0.73±0.04% ($p < 0.01$) in the CMC 100μg/ml group, and 0.67±0.07% ($p < 0.05$) in the CMC 1000μg/ml group.

The change in PADSCs is similar to that of the PDCs. After 48 hours of stimulation, the phosphorylation level of AMPK was 12.12±0.92% in the control group, increased to 19.02±1.22% ($p < 0.05$) in the CMC 10μg/ml group, to 19.27±1.19%($p < 0.01$) in the CMC 100μg/ml group, and 20.21±1.96%($p < 0.05$) in the CMC 1000μg/ml group. While the β-catenin/β-actin ratio was 0.51±0.02 in the control group, it increased to 0.78±0.06% ($p < 0.05$) in the CMC 10μg/ml group, to 0.74±0.05% ($p < 0.05$) in the CMC 100μg/ml group, and 0.76±0.08% ($p < 0.05$) in the CMC 1000μg/ml group. The cyclin D1/β-actin ratio was 0.38±0.05 in the control group, increased to 0.74±0.06% ($p < 0.05$) in the CMC 10μg/ml group, to 0.74±0.05%($p < 0.01$) in the CMC 100μg/ml group, and 0.83±0.04%($p < 0.01$) in the CMC 1000μg/ml group (Figure 5b).

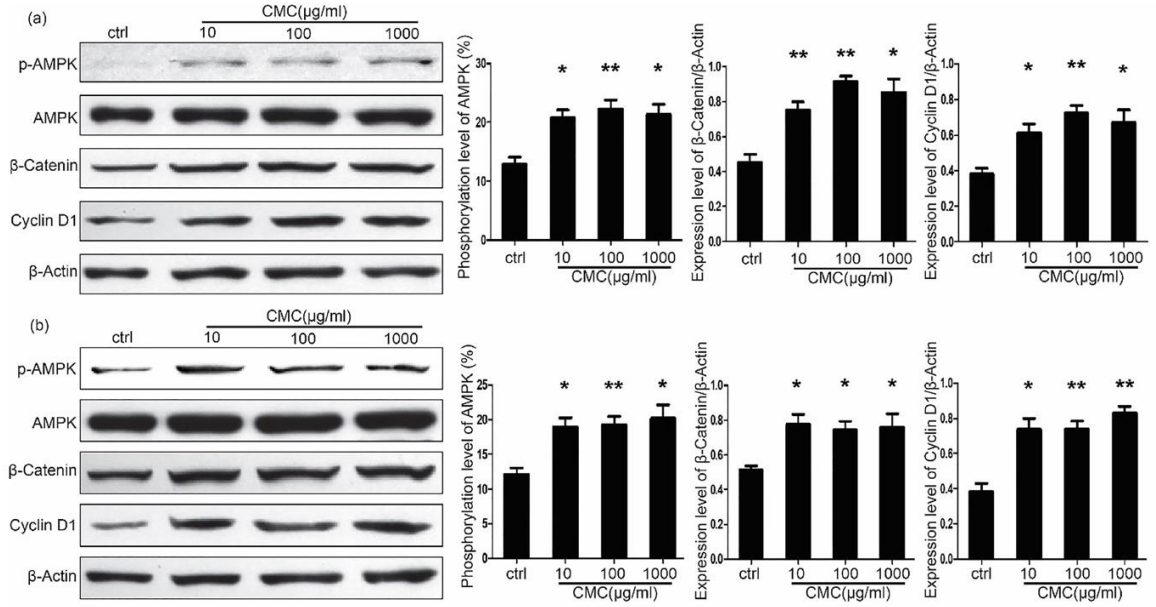

Figure 5: Cellular signaling affected by CMC in both PDCs and PADSCs. (a). CMC enhanced the phosphorylation of AMPK, which led to the accumulation of β-catenin and activated the Wnt/β-catenin signal pathway. This resulted in the increased expression of Cyclin D1 in PDCs. (b). Effect of CMC on PADSCs in vitro (n=3, error bars represent SD, *P< 0.05, **P< 0.01).

4. Discussion

A wound can be classified as "open" when the skin is torn, cut, or punctured, or "closed" when blunt force trauma causes a contusion. After any injury to skin, epithelization is an important event for wound healing, ensuring that new epithelium is formed in order to close the wound. Formation of a new epithelium requires the proliferation of keratinocytes, fibroblasts, dermal stem cells, and MSCs. Promoting cell differentiation and re-epithelialization, DSCs and MSCs are essential for skin homeostasis and repair of the wounds. In the past decades, research has proven that ADSCs are a good resource for tissue regeneration[18-22]. Subsequent studies combined CMC and ADSCs as a new strategy to treat skin wounds. Although the experiments clearly demonstrated that CMC plus ADSCs significantly enhanced tissue healing, the underlying mechanisms of this effect were not understood.

In our study, to test the effect on cell growth, CMC, BS, and BSiX (at a concentration of 156μg/ml) were used to treat PDCs for 24 hours. The results indicated that both CMC and BSiX promote PDC growth, especially BSiX; the effect from BS was minor. Then, we focused on CMC and BSiX. H3P and MTT results had similar trends, which means that both CMC and BSiX promote PDC mitosis and proliferation. We also assessed the dose-dependent responses using concentrations of 0, 10, 100 and 1000μg/ml of CMC and BSiX. This provides a reference for the selection of CMC and BSiX concentration for future use in experimental and clinical applications.

As CMC is the main ingredient of BSiX, then we investigated the mechanisms by which CMC activates cells. To do this we isolated and cultured PDCs and

PADSCs and then checked the signaling pathway in vitro, as dermal cells and stem cells play a very important role in the wound healing. It is well known that the Wnt/β-catenin signaling pathway is an evolutionarily conserved cellular signaling system that is involved in embryonic development [23, 24], cell proliferation, and differentiation [25-27]. Some Wnt proteins such as β-catenin may be key factors that regulate the rate of cell proliferation during the healing process [28]. After treatment with different concentrations of CMC, β-Catenin was significantly increased in both PDCs and PADSCs. This indicates that CMC can activate Wnt/β-catenin signaling pathway in both types of stem cells. After the activation of Wnt/β-catenin signaling pathway, the expression of cyclin D1 was consequently increased.

The next question is how CMC activates the Wnt/β-catenin signaling pathway. CMC is composed of glucopyranose subunits that have the ability to bind the glucose transporter (GLTU). When binding to glucose transporters, CMC competitively inhibits the intracellular transfer of glucose, which lowers the concentration glucose in cytoplasm and activates the AMPK pathway. AMPK, a critical regulator of energy metabolism [29-31], have been proved to promote β-catenin expression through phosphorylation of HDAC5 and phosphorylates β-catenin at Ser 552, which stabilizes β-catenin, enhances β-catenin/TCF mediated transcription [32, 33]. Then we checked the expression of p-AMPK and AMPK by Western blot. The results showed that different concentration of CMC can activate AMPK by increasing the ratio of p-AMPK/AMPK.

With these results in mind, we propose a hypothetical mechanism for CMC in activating DSCs and ADSC (Figure 6). As shown in figure 5, CMC can bind to GLTU to inhibit the intracellular transfer of glucose, which leads to low glucose concentrations in cytoplasm and then activates AMPK. AMPK can crosstalk with Wnt/β-catenin to promote the expression of downstream genes, such as H3P and Cyclin D1. This activates mitosis of stem cells and dermal cells to promote wound healing.

However, it should be cautioned that our study has limitations and that these findings require further validation. Our study just explored the mechanisms of CMC, the other type of CMC, such as BSiX need to be investigated in the futured study.

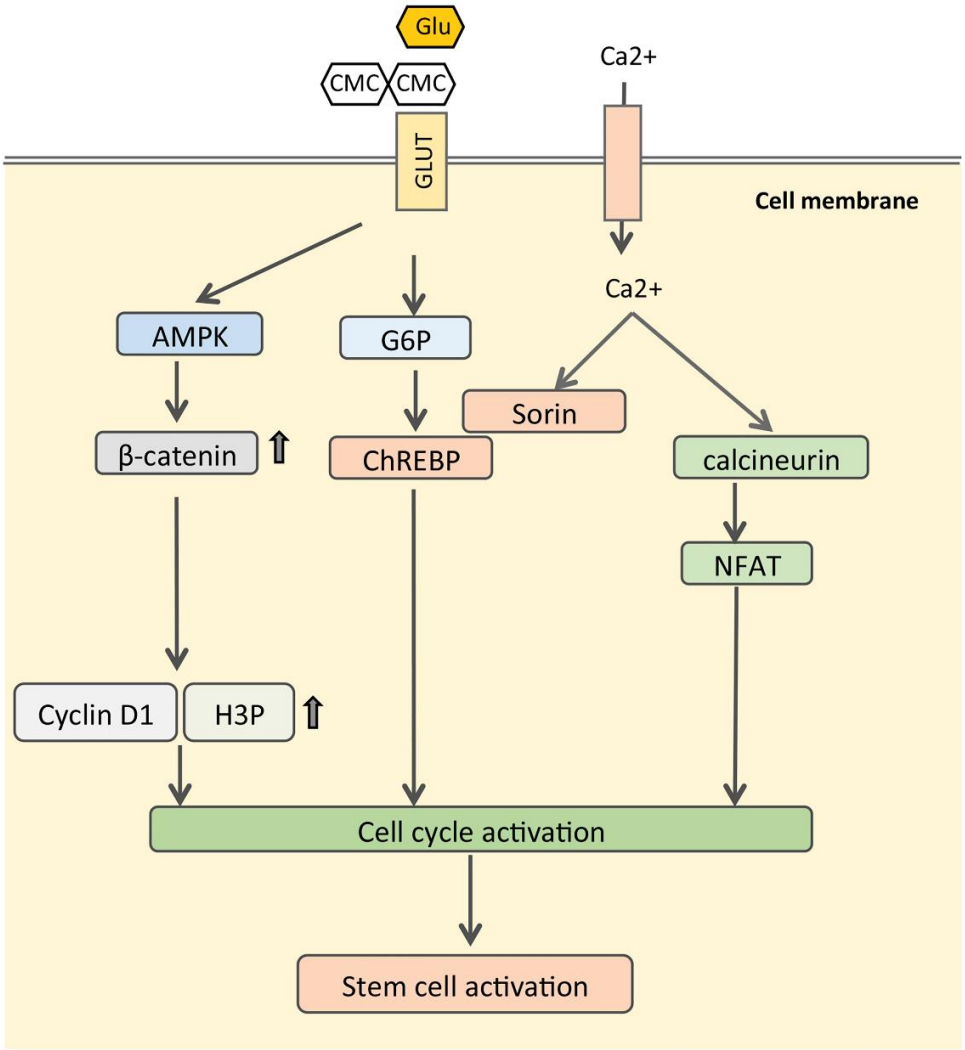

Figure 6: A hypothetical mechanism of CMC in activating DSCs and ADSCs

5. Conclusion

In this study, we isolated and cultured PDCs and PADSCs successfully. Both CMC and BSiX promoted mitosis and proliferation of PDCs in a dose-dependent manner. CMC activated Wnt//β-catenin signaling pathway through AMPK in both PDCs and PADSCs. This may be the mechanism by which CMC activates stem cells and dermal cells to promote wound healing.

References

1. Van Zuijlen PP, Vloemans JF, Van Trier AJ, Suijker MH, Van Unen E, Groenevelt F, et al. Dermal substitution in acute burns and reconstructive surgery: a subjective and objective long-term follow-up. Plast Reconstr Surg 108 (2001): 1938-1946.
2. Lipp C, Kirker K, Agostinho A, James G, Stewart P. Testing wound dressings using an in vitro wound model. J Wound Care 19 (2010): 220-226.
3. Liuyun J, Yubao L, Chengdong X. Preparation

and biological properties of a novel composite scaffold of nano-hydroxyapatite/chitosan/carboxymethyl cellulose for bone tissue engineering. J Biomed Sci 16 (2009): 65.

4. Rodrigues C, De Assis AM, Moura DJ, Halmenschlager G, Saffi J, Xavier LL, et al. New therapy of skin repair combining adipose-derived mesenchymal stem cells with sodium carboxymethylcellulose scaffold in a pre-clinical rat model. PLoS One 9 (2014): e96-241.
5. Gaihre B, Jayasuriya AC. Fabrication and characterization of carboxymethyl cellulose novel microparticles for bone tissue engineering. Mater Sci Eng C Mater Biol Appl 69 (2016): 733-743.
6. Ramli NA, Wong TW. Sodium carboxymethylcellulose scaffolds and their physicochemical effects on partial thickness wound healing. Int J Pharm 403 (2011): 73-82.
7. Liang M, Chen Z, Wang F, Liu L, Wei R, Zhang M. Preparation of self-regulating/anti-adhesive hydrogels and their ability to promote healing in burn wounds. J Biomed Mater Res B Appl Biomater 107 (2019): 1471-1482.
8. Calienno R, Curcio C, Lanzini M, Nubile M, Mastropasqua L. In vivo and ex vivo evaluation of cell-cell interactions, adhesion and migration in ocular surface of patients undergone excimer laser refractive surgery after topical therapy with different lubricant eyedrops. Int Ophthalmol 38 (2018): 1591-1599.
9. Garrett Q, Simmons PA, Xu S, Vehige J, Zhao Z, Ehrmann K, et al. Carboxymethylcellulose binds to human corneal epithelial cells and is a modulator of corneal epithelial wound healing. Invest Ophthalmol Vis Sci 48 (2007): 1559-1567.
10. Lai JC, Lai HY, Nalamolu KR, Ng SF. Treatment for diabetic ulcer wounds using a fern tannin optimized hydrogel formulation with antibacterial and antioxidative properties. J Ethnopharmacol 189 (2016): 277-289.
11. Piaggesi A, Baccetti F, Rizzo L, Romanelli M, Navalesi R, Benzi L. Sodium carboxyl-methyl-cellulose dressings in the management of deep ulcerations of diabetic foot. Diabet Med 18 (2001): 320-324.
12. Pasqui D, Torricelli P, De Cagna M, Fini M, Barbucci R. Carboxymethyl cellulose-hydroxyapatite hybrid hydrogel as a composite material for bone tissue engineering applications. J Biomed Mater Res A 102 (2014): 1568-1579.
13. Wang X, Tang P, Xu Y, Yang X, Yu X. In vitro study of strontium doped calcium polyphosphate-modified arteries fixed by dialdehyde carboxymethyl cellulose for vascular scaffolds. Int J Biol Macromol 93 (2016): 1583-1590.
14. Das A, Kumar A, Patil NB, Viswanathan C, Ghosh D. Preparation and characterization of silver nanoparticle loaded amorphous hydrogel of carboxymethylcellulose for infected wounds. Carbohydr Polym 130 (2015): 254-261.
15. Hebeish A, Hashem M, El-Hady MM, Sharaf S. Development of CMC hydrogels loaded with silver nano-particles for medical applications. Carbohydr Polym 92 (2013): 407-413.
16. Ogushi Y, Sakai S, Kawakami K. Adipose

tissue engineering using adipose-derived stem cells enclosed within an injectable carboxymethylcellulose-based hydrogel. J Tissue Eng Regen Med 7 (2013): 884-892.

17. Spera MBM, Taketa TB, Beppu MM. Roughness dynamic in surface growth: Layer-by-layer thin films of carboxymethyl cellulose/chitosan for biomedical applications. Biointerphases 12 (2017): 400-401.
18. Lin G, Garcia M, Ning H, Banie L, Guo YL, Lue TF, et al. Defining stem and progenitor cells within adipose tissue. Stem Cells Dev 17 (2008): 1053-1063.
19. Ning H, Lin G, Lue TF, Lin CS. Neuron-like differentiation of adipose tissue-derived stromal cells and vascular smooth muscle cells. Differentiation 74 (2006): 510-518.
20. Huang YC, Shindel AW, Ning H, Lin G, Harraz AM, Wang G, et al. Adipose derived stem cells ameliorate hyperlipidemia associated detrusor overactivity in a rat model. J Urol 183 (2010): 1232-1240.
21. Lin G, Wang G, Banie L, Ning H, Shindel AW, Fandel TM, et al. Treatment of stress urinary incontinence with adipose tissue-derived stem cells. Cytotherapy 12 (2010): 88-95.
22. Fandel TM, Albersen M, Lin G, Qiu X, Ning H, Banie L, et al. Recruitment of intracavernously injected adipose-derived stem cells to the major pelvic ganglion improves erectile function in a rat model of cavernous nerve injury. Eur Urol 61 (2012): 201-210.
23. Buckingham M. Skeletal muscle formation in vertebrates. Curr Opin Genet Dev 11 (2001): 440-448.
24. Tamura M, Nemoto E, Sato MM, Nakashima A, Shimauchi H. Role of the Wnt signaling pathway in bone and tooth. Front Biosci (Elite Ed) 2 (2010): 1405-1413.
25. Bienz M, Clevers H. Linking colorectal cancer to Wnt signaling. Cell 103 (2000): 311-320.
26. Pera MF, Tam PP. Extrinsic regulation of pluripotent stem cells. Nature 465 (2010): 713-720.
27. Nusse R, Clevers H. Wnt/beta-Catenin Signaling, Disease, and Emerging Therapeutic Modalities. Cell 169 (2017): 985-999.
28. Otto A, Schmidt C, Luke G, Allen S, Valasek P, Muntoni F, et al. Canonical Wnt signalling induces satellite-cell proliferation during adult skeletal muscle regeneration. J Cell Sci 121 (2008): 2939-2950.
29. Kim J, Solis RS, Arias EB, Cartee GD. Postcontraction insulin sensitivity: relationship with contraction protocol, glycogen concentration, and 5' AMP-activated protein kinase phosphorylation. J Appl Physiol (1985) 96 (2004): 575-583.
30. Hardie DG. AMP-activated protein kinase: a key system mediating metabolic responses to exercise. Med Sci Sports Exerc 36 (2004): 28-34.
31. Ruderman NB, Xu XJ, Nelson L, Cacicedo JM, Saha AK, Lan F, et al. AMPK and SIRT1: a long-standing partnership? Am J Physiol Endocrinol Metab 298 (2010): E751-E760.
32. Zhao J, Yue W, Zhu MJ, Sreejayan N, Du M. AMP-activated protein kinase (AMPK) cross-talks with canonical Wnt signaling via phosphorylation of beta-catenin at Ser 552. Biochem Biophys Res Commun 395 (2010): 146-1451.
33. Zhao JX, Yue WF, Zhu MJ, Du M. AMP-

activated protein kinase regulates beta-catenin transcription via histone deacetylase 5. J Biol Chem 286 (2011): 16426-16434.